Comparison of Static First Hyperpolarizabilities Calculated with Various Quantum Mechanical Methods

C. M. Isborn,[‡] A. Leclercq,[†] F. D. Vila,[§] L. R. Dalton,[‡] J. L. Brédas,[†] B. E. Eichinger,[‡] and B. H. Robinson*,[‡]

Department of Chemistry, University of Washington, Seattle, Washington 98195-1700, Department of Chemistry, Georgia Institute of Technology, 770 State Street Atlanta, Georgia 30332-0400, and Department of Physics, University of Washington, Seattle, Washington 98195-1560

Received: June 29, 2006; In Final Form: November 14, 2006

The prediction of nonlinear electro-optic (EO) behavior of molecules with quantum methods is the first step in the development of organic-based electro-optic devices. Typical EO molecules may require calculations with several hundred electrons, which prevents all but the fastest methods (semiempirical and density functional theory (DFT)) from being used for EO estimation. To test the reliability of these methods, we compare dipole moments, polarizabilities, and first-order hyperpolarizabilities for a wide range of structures of experimental interest with Hartree−Fock (HF), intermediate neglect of differential overlap (INDO), and DFT methods. The relative merits of molecules are consistently predictable with every method.

Introduction

Theory has been a crucial element in the design of organic molecules for nonlinear optical (NLO) applications for more than a decade. For example, Marder et al.,[1] showed that bond length alternation (BLA) is a useful structural guide for predicting the relative values of hyperpolarizabilities of a homologous series of molecules. A wealth of semiempirical, Hartree−Fock (HF), and density functional theory (DFT) calculations have been reported on a wide range of molecules; many hundreds of examples could be cited. Usually, the methods previously used have not been critically compared with one another. Exceptions to this statement are found, for example, in the work of Prezhdo,[2] Champagne et al.,[3] and Jacquemin et al.[4] The present study was undertaken as part of an ongoing collaborative effort to assess and develop theoretical tools to be used in the design of a new generation of NLO materials.

The molecules chosen for this study provide a wide range of structures and properties. The F*n* {$n = 1-4$} series (see Tables 1 and 2 for nomenclature and structures) was selected because these molecules have been found to have similar absorption spectra, yet they display a range of experimental hyper-Rayleigh scattering (HRS) behavior. The J4*n* series is identical to the J_{4n} series of Marder et al.[5] (denoted the J_{1n} series in the Lu et al.[6] paper), and J26 differs from that in the J_{2n} series of ref 4 by substitution of the two ethyl groups on the acceptor ring by two methyl groups. The last few entries, pNA, FTC, and CLD, YL181, and ZW18c, represent a range of structures having widely varying properties. The first, pNA, is one of the first molecules showing appreciable nonlinear optical behavior[7] and is frequently used as a standard. The molecules FTC[8,9] and CLD[10] are the benchmarks for families of chromophores being developed at the University of Washington. Finally, YL181 and ZW18c are of current interest;[11] they are of comparable size, with the latter being a zwitterion in the ground state. This set of molecules provides a test of consistency of the relative magnitude and sign of the second-order polarizability (or first-order hyperpolarizability) tensor, β, computed by the various methods.

The various electronic-structure methods were applied to exactly the same molecular geometries (except for those from the Lu et al.[6] work that we report). The methods in current usage within our respective groups and institutions are (i) intermediate neglect of differential overlap (INDO), (ii) Hartree−Fock (HF) with Gaussian basis sets, (iii) density functional theory (DFT) with Gaussian basis sets and the B3LYP functional, and (iv) DFT with numerical basis sets using the RPBE functional. These techniques have each proved useful as aids for molecular design, and here we address the issue of relative consistency among the methods. Our only concern is with isolated molecule (gas-phase) calculations. The important frequency dependence, condensed phase reaction field, and vibrational problems are beyond the scope of this work and therefore not addressed.

Definitions

The electrical response of a single molecule to an imposed static electric field results in the polarization of the molecule altering its dipole moment according to

$$\mu_i(\mathbf{F}) = \mu_i + \alpha_{ij}F_j + \frac{1}{2!}\beta_{ijk}F_jF_k + \frac{1}{3!}\gamma_{ijkl}F_jF_kF_l + \ldots \quad (1)$$

where the Einstein summation convention is used. Here the components of the imposed homogeneous electric field are the F_i terms, the dipole moment is $\mu_i(\mathbf{F})$ in the field and μ_i at zero field, the components of the polarizability tensor are $\alpha_{ij} = (\partial\mu_i/\partial F_j)_{\mathbf{F}=0}$, the components of the first-order hyperpolarizability are $\beta_{ijk} = (\partial^2\mu_i/\partial F_j\partial F_k)_{\mathbf{F}=0}$, the second-order hyperpolarizability components are γ_{ijkl}, and so on. Equation 1 is the Taylor series definition of the response, which differs from the power series definition by explicit incorporation of the $1/n!$ terms.

For isolated molecules, the dipole vector, $\mu_i(\mathbf{F})$, is the negative of the first derivative of the molecular energy, $E(\mathbf{F})$, with respect

* Author to whom correspondence and requests for reprints should be addressed.
[‡] Department of Chemistry, University of Washington.
[†] Department of Chemistry, Georgia Institute of Technology.
[§] Department of Physics, University of Washington.

10.1021/jp064096g CCC: $37.00
Published on Web 01/26/2007

TABLE 1: Molecules and Their Geometries

Designation and Structure	Geometry
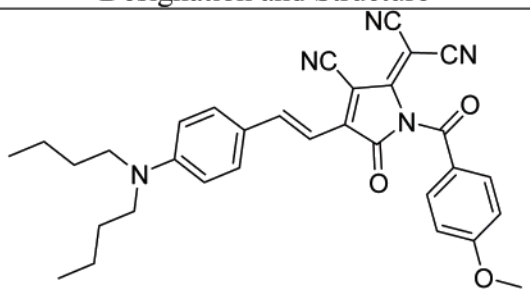 F1	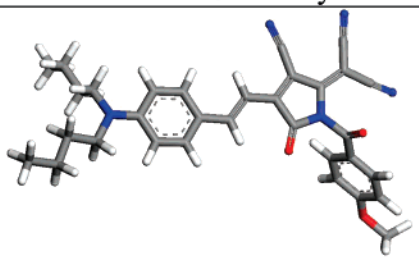
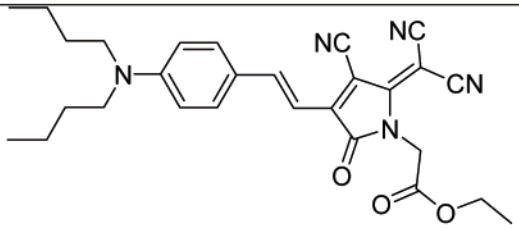 F2	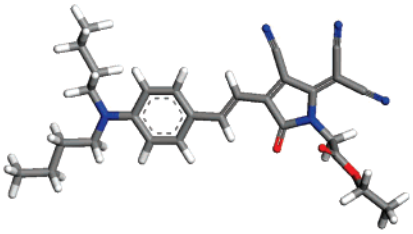
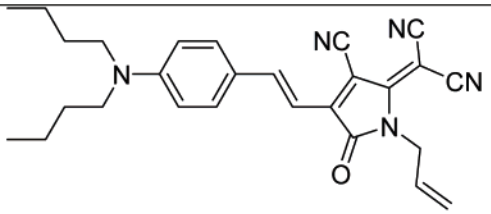 F3	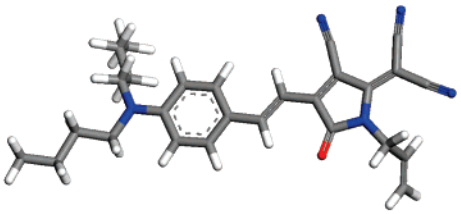
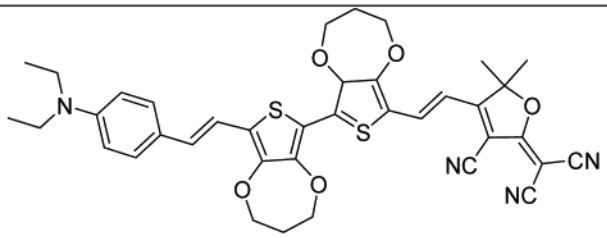 F4	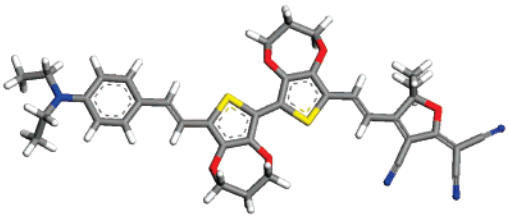
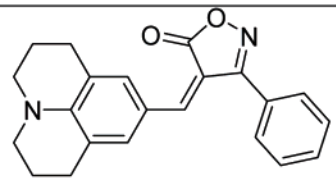 J40	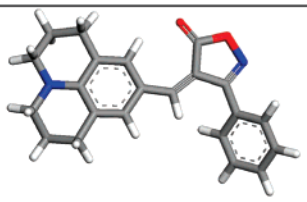
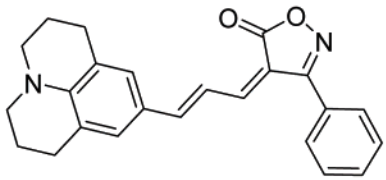 J41	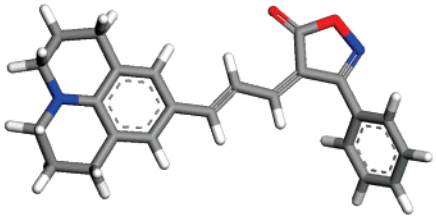
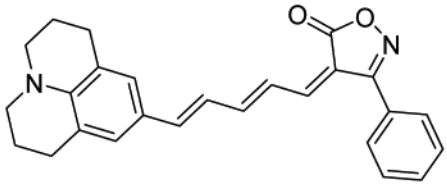 J42	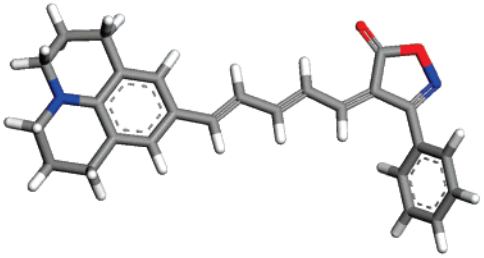

TABLE 1: (Continued)

Designation and Structure	Geometry
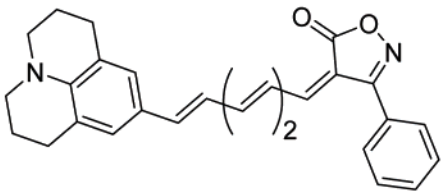 J43	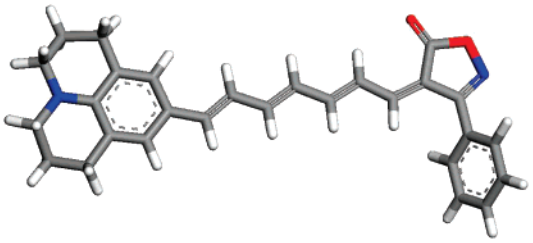
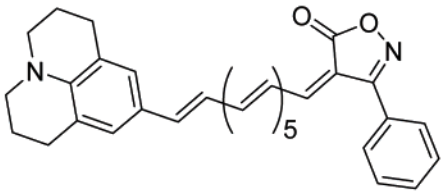 J46	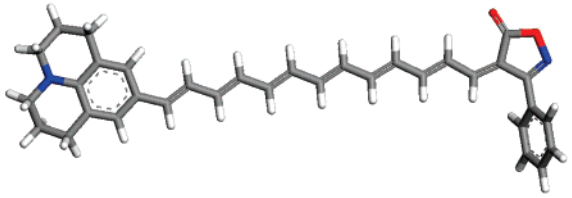
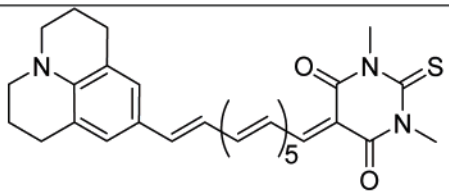 J26	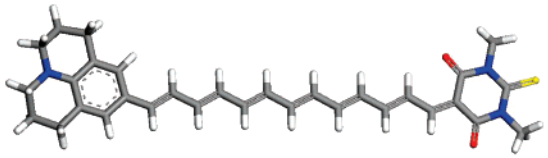
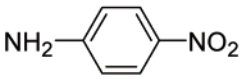 PNA	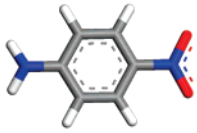
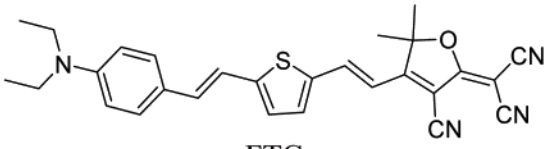 FTC	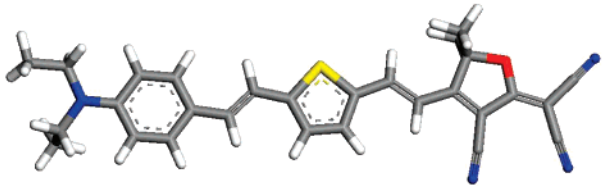
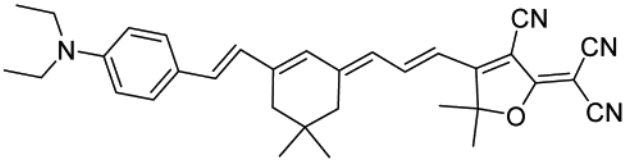 CLD	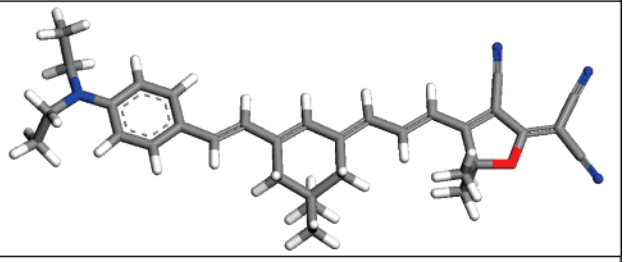
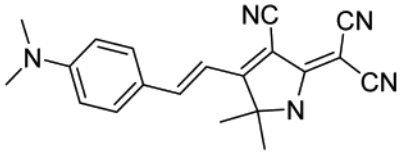 YL-181	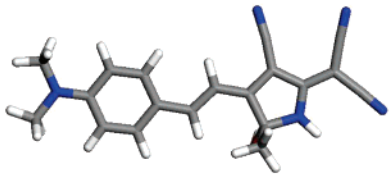
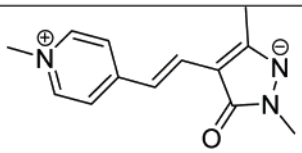 ZW-18c	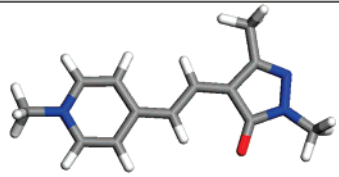

TABLE 2: Molecule Designation and IUPAC Names

F1	2-[3-cyano-4-[2-(4-(dibutylamino)phenyl)vinyl]-1-(4-methoxybenzoyl)-5-oxo-1,5-dihydropyrrol-2-ylidene]-malononitrile
F2	{3-cyano-2-(dicyanomethylene)-4-[2-(4-(dibutylamino)phenyl)vinyl]-5-oxo-2,5-dihydropyrrol-1-yl}-acetic acid ethyl ester
F3	2-{1-allyl-3-cyano-4-[2-(4-(dibutylamino)phenyl)vinyl]-5-oxo-1,5-dihydropyrrol-2-ylidene}-malononitrile
F4	2-[3-cyano-4-(2-{8′-[2-(4-(diethylamino)phenyl)vinyl]-3,4,3′,4′-tetrahydro-2*H*,2′*H*-[6,6′]bis[thieno[3,4-*b*][1,4]dioxepinyl]-8-yl}vinyl)-5,5-dimethyl-5*H*-furan-2-ylidene]-malononitrile
J40	3-phenyl-4-(2,3,6,7-tetrahydro-1*H*,5*H*-pyrido[3,2,1-*ij*]quinolin-9-ylmethylene)-4*H*-isoxazol-5-one
J41	3-phenyl-4-[3-(2,3,6,7-tetrahydro-1*H*,5*H*-pyrido[3,2,1-*ij*]quinolin-9-yl)-allylidene]-4*H*-isoxazol-5-one
J42	3-phenyl-4-[5-(2,3,6,7-tetrahydro-1*H*,5*H*-pyrido[3,2,1-*ij*]quinolin-9-yl)-penta-2,4-dienylidene]-4*H*-isoxazol-5-one
J43	3-phenyl-4-[7-(2,3,6,7-tetrahydro-1*H*,5*H*-pyrido[3,2,1-*ij*]quinolin-9-yl)-hepta-2,4,6-trienylidene]-4*H*-isoxazol-5-one
J46	3-phenyl-4-[13-(2,3,6,7-tetrahydro-1*H*,5*H*-pyrido[3,2,1-*ij*]quinolin-9-yl)-trideca-2,4,6,8,10,12-hexaenylidene]-4*H*-isoxazol-5-one
J26	1,3-dimethyl-5-[13-(2,3,6,7-tetrahydro-1*H*,5*H*-pyrido[3,2,1-*ij*]quinolin-9-yl)-trideca-2,4,6,8,10,12-hexaenylidene]-2-thioxodihydropyrimidine-4,6-dione
pNA	4-nitrophenylamine or *para*-nitroaniline
FTC	2-[3-cyano-4-(2-{5-[2-(4-(diethylamino)phenyl)vinyl]thiophen-2-yl}vinyl)-5,5-dimethyl-5*H*-furan-2-ylidene]-malononitrile
CLD	2-[3-cyano-4-(3-{3-[2-(4-(diethylamino)phenyl)vinyl]-5,5-dimethylcyclohex-2-enylidene}-propenyl)-5,5-dimethyl-5*H*-furan-2-ylidene]-malononitrile
YL181	2-{3-cyano-4-[2-(4-(dimethylamino)phenyl)vinyl]-5,5-dimethyl-1,5-dihydropyrrol-2-ylidene}-malononitrile
ZW18c	2,5-dimethyl-4-[2-(1-methylpyridinium-4-yl)vinyl]pyrazol-3-on-1-ide

to the field components (Hellmann−Feynman theorem). This applies in the case where the fields are time independent and the external field part of the Hamiltonian is $H_{opt} = -\hat{\mu}\cdot\vec{F}$; then $\mu_i = -\partial E(F)/\partial F_i = -\langle \partial H_{opt}/\partial F_i \rangle = \langle \partial \hat{\mu}\cdot\vec{F}/\partial F_i \rangle = \langle \hat{\mu}_i \rangle$. Comparison with eq 1 leads to an alternative definition of the electrostatic moments via the Taylor series

$$E(\mathbf{F}) = E(0) - \mu_i F_i - \frac{1}{2!}\alpha_{ij}F_iF_j - \frac{1}{3!}\beta_{ijk}F_iF_jF_k - ... \quad (2)$$

where the coefficients, i.e., derivatives of the energy, are evaluated at zero field. In this version, the (Kleinman[12]) symmetry of the tensors is clear.

The primary focus of this work is on the first-order hyperpolarizability, and we report values in the convention of eq 1. (Note that vectors and tensors, with their implicit (Cartesian) basis, will be denoted by boldface letters, and their components will be denoted by the same letters in subscript Italics.) However, dipole moments and polarizabilities will also be reported: the magnitude of the former is simply μ, and α is $^1/_3$ the trace of the polarizability tensor. In general, the phenomenological coefficients (α and higher) on the right in eq 1 are frequency dependent; however, we are here concerned only with the static properties.

Experimental measures of the first-order hyperpolarizability, simply referred to as the hyperpolarizability for our purposes, include hyper-Rayleigh scattering (HRS), electric-field dependence of refractive index (r_{ij}), and electric field induced second harmonic generation (EFISH). Computational methods generally give most, if not all, of the unique components of the hyperpolarizability tensor, and for comparison with experiments various scalar measures of the tensors need to be computed. One of the simplest such scalars, though not directly given by experiments, is the average

$$\langle\beta\rangle = \sqrt{{\beta_1}^2 + {\beta_2}^2 + {\beta_3}^2} \quad (3)$$

where

$$\beta_i = \frac{1}{3}\sum_{j=1}^{3}(\beta_{ijj} + \beta_{jij} + \beta_{jji}) = \sum_{j=1}^{3}\beta_{ijj} \quad (4)$$

with the final version resulting from Kleinman symmetry. (Here we show explicit sums, rather than the summation convention, to conform to standard practice.) The average required for interpretation of EFISH measurements is β_μ (sometimes denoted by $\beta_{||}$), the strength of the hyperpolarizability in the direction of the dipole moment, which is defined by

$$\beta_\mu = \frac{\sum_{i=1}^{3}\mu_i\beta_i}{|\mu|} \quad (5)$$

The measures of hyperpolarizability provided by eqs 3 and 5 will be the focus of our discussions.

Methods

The various methods are identified in the tables and figures by shorthand notations. Calculations were done using: (1) the RPBE functional in DMol[3], (2) a modified ZINDO code labeled INDO, and Gaussian03 for both (3) HF and (4) B3LYP calculations. Results from the literature obtained by the Goddard group using the (5) PS-GVB code (actually a HF method) are so indicated. Further details on the methods are as follows:

RPBE

The geometries of all molecules were optimized using the DMol[3] code[13,14] with the RPBE[15] functional and the best available numerical basis set (dnp: this basis set uses approximately twice as many atomic orbitals as are occupied in the isolated atoms, plus polarization functions on all atoms, including H). Geometry convergence required that two out of three conditions are satisfied: energy to 2×10^{-5} hartrees, maximum force to 0.004 hartree/Å, or maximum displacement to 0.005 Å. Numerical integrations were performed on a medium grid using the default octupolar option with radial integrals truncated at 5.5 Å. These structures, given in Table 1, were used without modification for all subsequent calculations done with the various methods.

Calculations of electrostatic moments with DMol[3] were performed using the finite field method. Fields of strength ϵ and 2ϵ, with $\epsilon = 0.001$ au (1 au of field corresponds to 5.14×10^9 V/cm), were applied along the $\pm x$, $\pm y$, and $\pm z$ directions, which together with the zero field result gave 13 dipole vectors that were analyzed by the method of Sim et al.,[7] to extract the polarizability and hyperpolarizability. (Calculations done for a range of field strengths for small molecules,[16] including *p*-nitroaniline, showed that fields of this magnitude generally gave good results as judged by the symmetry of the polarizability and first hyperpolarizability tensors. Field strengths in this range have been successfully used heretofore for several INDO

calculations of molecules of comparable size,[17−19] and furthermore, a field strength of 0.001 au is the default setting in Gaussian03 (see below). For molecules with much larger hyperpolarizabilities, smaller finite fields will be required to avoid contamination from higher order hyperpolarizabilities when using this method of data analysis.) For these calculations, the precision was increased by setting the integration grid to *fine*, with radial integrations truncated at 7.0 Å, and energies converged to 1×10^{-6} Ha. (Calculations with cutoffs ranging from 5.0 to 8.0 Å showed that the dipole moment of pNA at 7.0 A had converged to within 0.0005 D of its value at 8.0 Å, and this was judged to be sufficiently accurate for the difference calculations required to extract the polarizabilities and first hyperpolarizabilities of the molecules investigated here.)

INDO

The electronic properties (state dipole moments, transition dipole moments, and transition energies) were evaluated from the semiempirical INDO[20] Hamiltonian. The spectroscopic parametrization and the Mataga−Nishimoto[21] electron repulsion scheme were used, as implemented in the ZINDO[22] code. The INDO calculation was coupled to a single configuration interaction (SCI) scheme, which is known to give a reliable description of the properties of one-photon allowed excited states, which are those involved in the perturbative description of the first-order hyperpolarizability.[23] The 30 highest occupied and 30 lowest unoccupied molecular orbitals were active in the SCI procedure. Results are essentially converged at the 30×30 level, as was routinely tested against larger calculations.

The molecular polarizabilities and hyperpolarizabilities were calculated using the sum-over-states (SOS)[24] method, which uses standard perturbation equations with excitation energies, transition dipole moments, and state dipole moments obtained from the INDO/SCI calculations.

HF and B3LYP

The Gaussian03 program suite[25] was used for all HF and B3LYP[26] calculations. Because a large basis set is important for optical properties,[27] both diffuse and polarization functions were included via the Pople 6-31+G(d,p) basis. Calculations were performed with analytic derivatives in the HF method, and numerical derivatives were used in the finite field method with B3LYP to obtain the hyperpolarizability. With numerical derivatives, the default method of applying an electric field of 0.001 atomic units (au) along the Cartesian directions was used, or an external electric field was created with two opposite point charges of $\pm 500e$ at 1000 Bohr on either side of the molecule along the *x*, *y*, and *z* axes to create the same field strength of 0.001 au. Polarizabilities and hyperpolarizabilities were computed from central differences. HF and B3LYP calculations converged the root-mean square (rms) error in the density matrix to at least 10^{-7} and the energy to 10^{-5} au (only one molecule, J13, did not converge to 10^{-8} and 10^{-6}, respectively).

PS-GVB

The results under this heading were taken from the paper of Lu et al.[6] They used the 6-31G basis set for HF calculations with their PS-GVB code. Their geometries were obtained from X-ray crystallography or were pieced together from X-ray structural components and HF-geometry optimized moieties. Favorable comparisons with the experiments of Marder et al.[5] are provided in that work.

Results

Table 3 summarizes the results obtained with the various methods. Part a contains dipole moments, μ, and polarizabilities, $\alpha = (1/3)\mathrm{Tr}(\alpha)$, and part b displays the measures β_μ and $\langle\beta\rangle$ of the first-order hyperpolarizabilities that were computed using eqs 3−5. The entries under the PS-GVB columns were computed by our using the components of the hyperpolarizability tensors provided in the published work of Lu et al.[6] Figures showing the relative results for μ (Figure 1), α (Figure 2), and the two measures of β (Figures 3 and 4) are also given.

The correlation diagram for the dipole moments (Figure 1) shows that the INDO results generally lie well below the values for all other methods, the exceptions being pNA and ZW18c. The two DFT methods, B3LYP and RPBE, agree quite well with one another, and tend to predict slightly larger μ than HF. The HF method implemented in the PS-GVB code tracks Gaussian03 HF very well, with the exception of the larger molecules J46 and J26, which are anomalously low relative to the Gaussian03 HF line. RPBE and B3LYP depart from HF in the positive direction by similar amounts for these two molecules. (Our choice of HF as the basis for comparison in our correlation diagrams should not be construed as an endorsement of this method over another: HF is a traditional or conventional choice.)

The linear polarizabilities, α, follow the same general trends as the dipole moments, as the INDO polarizabilities are low relative to HF, and the DFT values are a little higher. The calculated α values from INDO are consistently about 70% of the HF values, and the DFT results are never more than about 36% larger. The deviation between DFT and HF polarizabilities increases as the magnitude of α increases, which parallels the finding of Jacquemin et al.[4] in their studies of oligo(methineimines). They found that the relative difference between DFT and HF estimates of the longitudinal components of the polarizabilities of the homologous series increased as the magnitude of the polarizability increased. They argued[4,28] that the deviation arises from the local nature of the DFT exchange functionals. Regardless of relative differences between methods, within a given method the trends are consistent, and our results lend considerable confidence to one's ability to compute average vacuum polarizabilities to within 10−20% of one another with these methods for molecules of the size considered here.

Hyperpolarizabilities computed with the various methods are, surprisingly, just as closely correlated with one another as are the lower electrostatic moments, as inspection of Figures 3 and 4 reveals. The INDO values are quite similar to HF values, except for pNA, ZW18c and J40. B3LYP values are consistently higher than HF in the β_μ measure, and RPBE gives a somewhat steeper slope in this correlation diagram (Figure 3). The estimates of β with DFT are approximately 30−70% larger than with HF for the largest hyperpolarizabilities, which is within the range of differences seen by Jacquemin et al.[4] in their study of oligo(methineimines). The $\langle\beta\rangle$ and β_μ values computed with the two DFT methods agree very closely with one another over the entire range of molecules in this set when compared for absolute, not relative, differences.

The trends just described have been observed before, and DFT has been criticized for overestimating hyperpolarizabilities for highly active molecules. In a series of publications on push−pull molecules and several different oligomeric systems, Champagne, Jacquemin, and co-workers[3,4,29] have implicated inadequate screening in DFT in the overestimation of both dipole moments and hyperpolarizabilities in long conjugated molecules. It appears from their work[4] that the most important structural feature that DFT gets wrong is bond-length alternation. Inspection of Figure 6 of ref 4, as well as the authors' discussion, shows that even MP2 begins to overestimate the longitudinal

TABLE 3: Results Obtained for the Molecules of Table 1

(a) Dipole Motcments (Debyes) and Polarizabilities (Å^3)

	μ					α			
molecule	RPBE	INDO	HFy	B3LYP	PS-GVB	RPBE	INDO	HF	B3LYP
F1	17.3	11.5	16.4	16.7		96	50	80	95
F2	17.4	11.3	16.5	16.8		87	45	73	86
F3	17.7	11.0	16.6	17.1		84	45	70	83
F4	27.5	19.6	25.5	26.4		169	84	122	159
J40	11.2	10.7	11.0	11.1	10.7	48	28	44	50
J41	13.3	11.4	12.5	13.0	12.5	61	36	54	62
J42	16.2	13.2	14.9	15.7	15.5	78	45	66	78
J43	18.2	14.0	16.3	17.6	16.7	99	57	80	97
J46	24.0	16.0	19.6	22.7	17.7	185	99	134	177
J26	23.4	18.7	20.8	23.6	15.3	201	105	142	194
pNA	7.5	8.0	7.5	7.5		15	13	14	15
FTC	26.0	18.2	24.6	25.2		120	66	90	114
CLD	28.4	21.7	28.0	27.9		138	73	107	133
YL181	18.1	13.9	18.1	17.8		60	35	50	59
ZW18c	10.8	12.4	12.5	11.4		37	31	36	38

(b) Scalar Polarizabilities β_μ and $\langle\beta\rangle$ (10^{-30} esu)

	β_μ				$\langle\beta\rangle$				
molecule	RPBE	INDO	HF	B3LYP	RPBE	INDO	HF	B3LYP	PS-GVB
F1	270	297	212	310	322	367	259	369	
F2	280	308	216	316	314	381	252	354	
F3	282	332	218	323	306	371	246	351	
F4	1630	685	655	1535	1754	827	740	1665	
J40	43	75	33	47	53	116	49	60	68
J41	111	138	83	129	129	211	112	154	120
J42	226	239	163	268	249	321	200	300	234
J43	409	366	293	493	440	471	343	537	464
J46	1491	923	1063	1891	1549	1099	1164	1980	884
J26	1706	1401	1403	2180	1713	1439	1416	2189	912
pNA	14	45	8	15	14	46	8	15	
FTC	819	522	476	783	845	553	502	818	
CLD	623	427	515	727	684	514	574	777	
YL181	117	126	89	141	132	161	106	157	
ZW18c	−20	−33	−22	−15	20	45	24	16	

hyperpolarizability of oligo(methineimines) at lengths greater than about 12 (CH═N) units when structures are optimized with either B3LYP or PBE0.

Hyperpolarizabilities calculated with MP2 but with molecular geometries optimized with MP2 or HF show much less rapid rise in β as chain length increases. This result suggests that it is most important to get the zero-field geometry right. If the structural method gives too little bond-length alternation, values of β will be overestimated, presumably no matter what method is used for calculation of the hyperpolarizability. Given that our DFT results for the largest molecules in this study show positive departures from HF, we need to look more closely at the relation between molecular dimensions and screening.

The shortest molecule in this study, J40, has just four conjugated single−double bond pairs between donor N atom and acceptor N atom, whereas the longest molecule, J46, has 10 such conjugated bond pairs. It can be inferred from the work of Champagne et al.,[3] that there is a crossover as one increases the chain length in the series $H_2N(CH{=}CH)_nNO_2$ between the domain where β(MP2) > β(B3LYP), found for $n = 6$, and the domain where β(MP2) < β(B3LYP) for $n = 12$ (their geometries were optimized with MP2/6-31G). Our molecules straddle the $n = 6$ oligomer in size. If the trends seen in the Champagne work can be translated to this more diverse set of molecules, then it may be inferred that we are mostly in a "safe" domain where none of the several methods used here can be unequivocally asserted to overestimate hyperpolarizabilities relative to MP2. However, the fact that the B3LYP hyperpolarizabilities for the largest molecules are larger than HF by about 50% is consistent with the Jacquemin et al.[4] results for $n = 10$ (their Figure 6). It is interesting that for J46 and J26, RPBE (without exact exchange) gives smaller hyperpolarizabilities than does B3LYP (with 20% exact exchange). This result is consistent with the Champagne et al.[3] result for $n = 6$ (comparing BLYP and B3LYP in Table 3 of their work) but is inconsistent with a similar comparison for $n = 12$. This again supports the claim that we are in the "safe" domain. We believe that the delicate tradeoff between geometry, exchange correlation, and screening requires yet more study to fully understand their implications for practical work. Although MP2 calculations would be desirable for molecules of the class considered here, this method is far too costly to use routinely. In fact, it has proved difficult for us to get an MP2 SCF cycle to converge for the geometry of FTC used here. As stated in the Introduction, more accurate methods, exemplified by MP2, are impractical for these molecules.

The sum-over-states method used with INDO gives hyperpolarizabilities for the largest molecules of our series that are nearer the HF results than either of the DFT methods, despite the generally poorer agreement for dipole moments and linear polarizabilities. We recall that, as used here, INDO is the only method coupled to an SOS scheme to evaluate the polarizabilities; in this instance, the β values are determined by the combination of three ingredients: squares of transition dipole moments, difference in dipole moment between the excited state and ground state, and square of transition dipoles. This combination turns out to provide β values close to the finite-field HF values. We note that, if an SOS-HF method were to

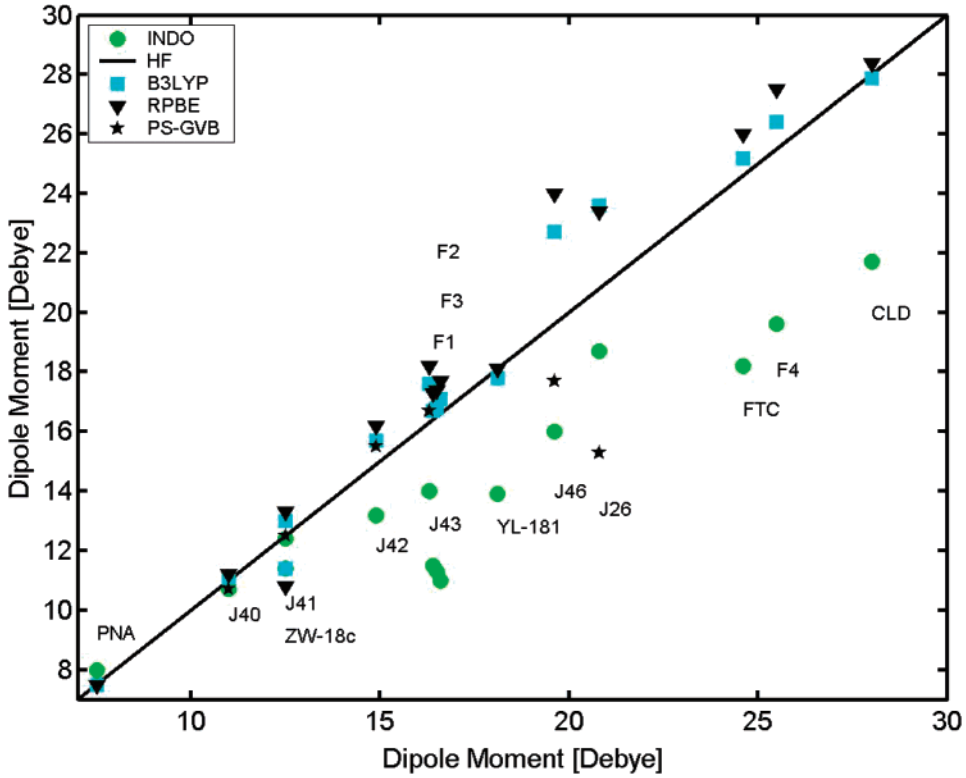

Figure 1. Dipole moments calculated with the methods indicated. The diagonal of the correlation diagram is the arbitrary standard, chosen to be HF for this and all subsequent plots.

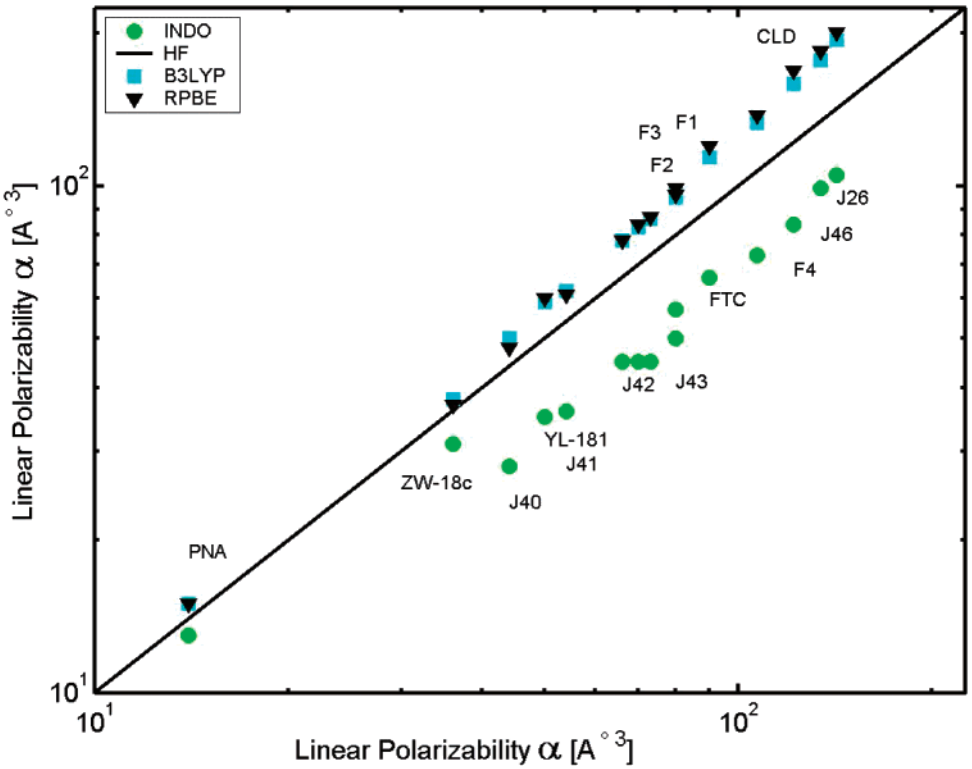

Figure 2. Polarizabilities calculated with the methods indicated by the inset. Again the diagonal is provided by HF. This measure of polarizability is 1/3 the trace of the polarizability tensor.

be used, the calculated β values would be expected to be consistently lower than the corresponding finite-field HF (because SOS is a perturbative and not a self-consistent-field approach).

Conclusions

The general trends shown in these calculations lead one to a few observations that should be of general interest. In the first

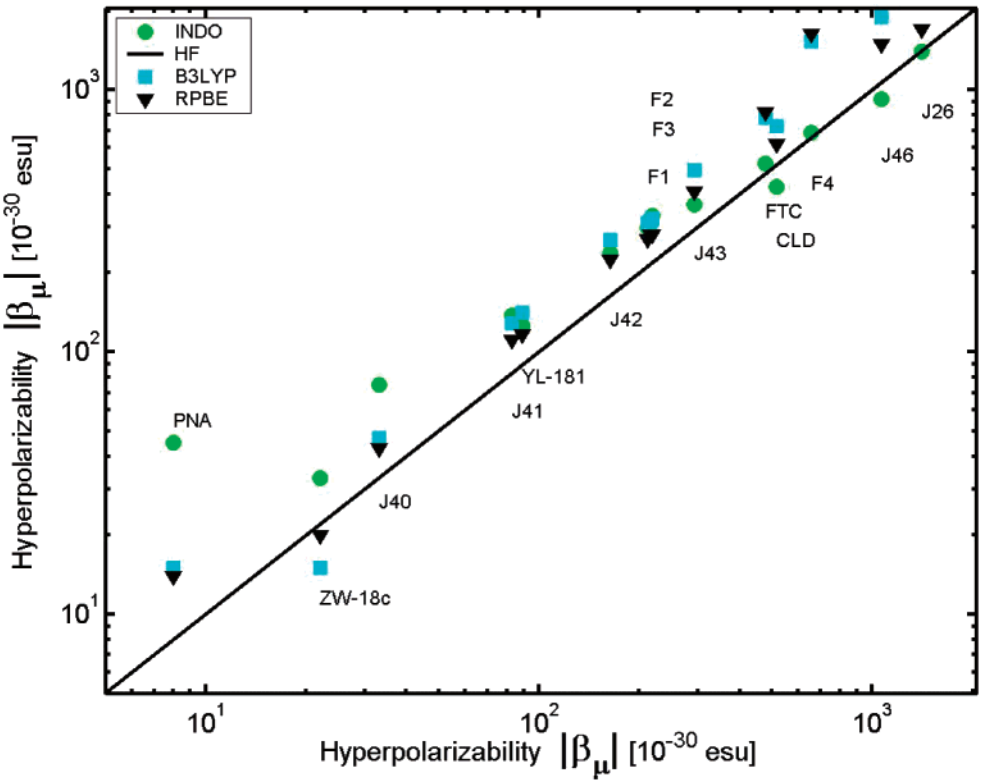

Figure 3. This measure of the hyperpolarizability is appropriate for EFISH and is calculated from the hyperpolarizability tensor as described in the text. The logarithm of the absolute values are plotted to accommodate the data for ZW18c, for which all methods give a negative β_μ as Table 3b shows.

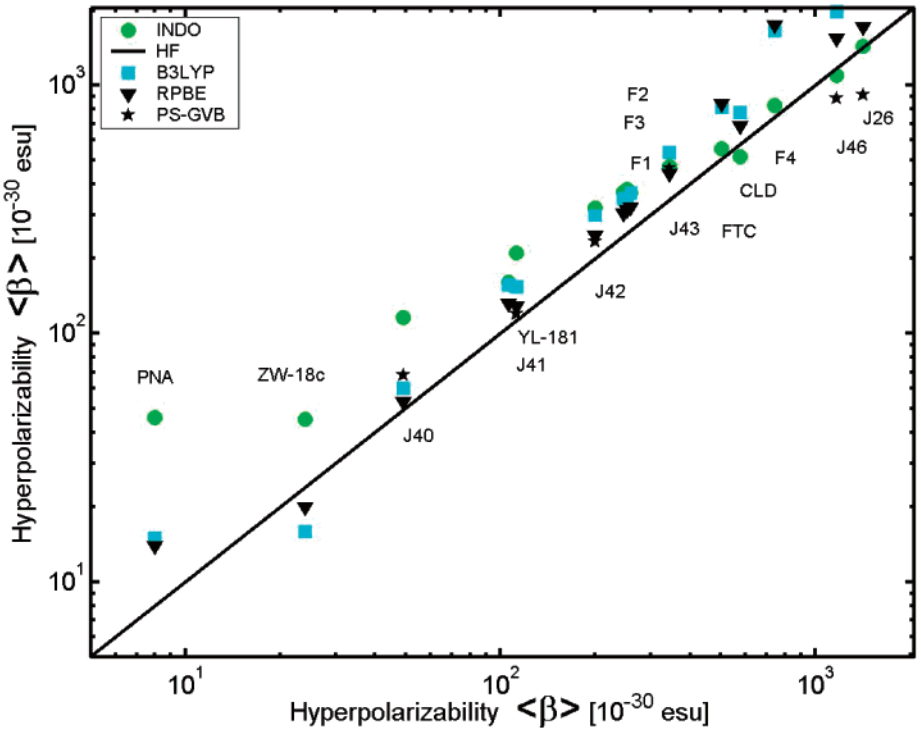

Figure 4. Average hyperpolarizability as defined by eq 3 of the text.

place, when used for screening in support of synthetic efforts, there is little to recommend one method over another. It is seen that the various methods, semiempirical, self-consistent field, and density functional, all give relatively consistent descriptions of the electrostatic moments for a wide variety of molecules having widely different properties, even for hyperpolarizabilities spanning several orders of magnitude. When used carefully and consistently, any one of the methods should provide useful guidance for an experimental program. This statement, of course, makes no claim for the absolute accuracy of any of the methods used here. It may be noted that relative values of hyperpolarizabilities computed with DMol[3] for molecules comparable to those studied here have been successfully correlated with experimental data,[30] and the absolute values calculated for

smaller molecules using B3LYP with extrapolated basis sets agree very well with experiment.[16]

The consistent discrepancy between values of β calculated by DFT and HF for the most active molecules merits further investigation. This is a very difficult problem, as other methods that might be used for standardization, such as Møller−Plesset perturbation theory (MPn) or coupled-cluster (CC) methods, rapidly become too expensive as the size of the molecule increases. Comparison with experimental results for these systems also includes the complications of condensed phase effects, which by current theory induce changes in calculated β values of factors of two or more. Calculation of the frequency dependence can be done with SOS methods or with time-dependent density functional theory (TD-DFT) methods under development.[31] Functionals that are designed to handle external fields also need to be explored for practical applications.[32,33]

Acknowledgment. Research support is gratefully acknowledged from the National Science Foundation Center on Materials and Devices for Information Technology Research (CMDITR), DMR-0120967. Additional support from the Air Force Office of Scientific Research and the Office of Naval Research is gratefully acknowledged.

References and Notes

(1) Marder, S. R.; Beratan, D. N.; Cheng, L.-T. *Science* **1991**, *252*, 103.

(2) Prezhdo, O. V. *Adv. Mater.* **2002**, *14*, 597.

(3) Champagne, B.; Perpete, E. A.; Jacquemin, D.; van Gisbergen, S. J. A.; Baerends, E. J.; Soubra-Ghaoui, C.; Robins, K. A.; Kirtman, B. *J. Phys. Chem. A* **2000**, *104*, 4755.

(4) Jacquemin, D.; Andre, J.-M.; Perpete, E. A. *J. Chem. Phys.* **2004**, *121*, 4389.

(5) Marder, S. R.; Cheng, L.-T.; Tiemann, B. G.; Friedli, A. C.; Blanchard-Desce, M.; Perry, J. W.; Skindhoj, J. *Science* **1994**, *263*, 511.

(6) Lu, D.; Marten, B.; Cao, Y., Ringnalda, M. N.; Friesner, R. A.; Goddard, W. A., III. *Chem. Phys. Lett.* **1995**, *242*, 543.

(7) Sim, F.; Chin, S.; Dupuis, M.; Rice, J. E. *J. Phys. Chem.* **1993**, *97*, 1158.

(8) Robinson, B. H.; Dalton, L. R.; Harper, A. W.; Ren, A.; Wang, F.; Zhang, C.; Todorova, G.; Lee, M.; Aniszfeld, R.; Garner, S.; Chen, A.; Steier, W. H.; Houbrecht, S.; Persoons, A.; Ledoux, I.; Zyss, J.; Jen, A. K. Y. *Chem. Phys.* **1998**, *245*, 35.

(9) Steier, W. H.; Chen, A.; Lee, S.-S.; Garner, S.; Zhang, H.; Chuyanov, V.; Dalton, L. R.; Wang, F.; Ren, A. S.; Zhang, C.; Todorova, G.; Harper, A. W.; Fetterman, H. R.; Chen, D.; Udupa, A.; Bhattacharya, D.; Tsap, B. *Chem. Phys.* **1999**, *245*, 487.

(10) Zhang, C.; Wang, C.; Yang, J.; Dalton, L. R.; Sun, G.; Zhang, H.; Steier, W. H. *Macromolecules* **2001**, *34*, 235.

(11) Liao, Y. Personal communication.

(12) Kleinman, D. A. *Phys. Rev.* **1962**, *126*, 1977.

(13) Delley, B. DMol, a Standard Tool for Density Functional Calculations: Review and Advances. In *Modern Density Functional Theory: A Tool for Chemistry*; Seminario, J. M., Politzer, P., Ed.; Elsevier Science Publishers: Amsterdam, 1995; Vol. 2.

(14) *Materials Studio and DMol3*; Accelrys: San Diego, 2002.

(15) Hammer, B.; Hansen, L. B.; Norskov, J. K. *Phys. Rev. B* **1999**, *59*, 7413.

(16) Davidson, E. R.; Eichinger, B. E.; Robinson, B. H. *Opt. Mater.* **2006**, *29*, 360.

(17) Geskin, V. M.; Bredas, J.-L. *J. Chem. Phys.* **1998**, *109*, 6163.

(18) Geskin, V. M.; Lambert, C.; Bredas, J.-L. *J. Am. Chem. Soc.* **2003**, *125*, 15651.

(19) Jacquemin, D.; Beljonne, D.; Champagne, B.; Geskin, V. M.; Bredas, J.-L.; Andre, J.-M. *J. Chem. Phys.* **2001**, *115*, 6766.

(20) Pople, J. A.; Beveredge, D. L.; Dobosh, P. A. *J. Chem. Phys.* **1967**, *47*, 2026.

(21) Mataga, N.; Nishimoto, K. *Z. Phys. Chem.* **1957**, *13*, 140.

(22) Zerner, M. C.; Loew, G. H.; Kichner, R. F.; Mueller-Westerhoff, U. T. *J. Am. Chem. Soc.* **1980**, *102*, 589.

(23) Meyers, F.; Marder, S. R.; Pierce, B. M.; Bredas, J.-L. *J. Am. Chem. Soc.* **1994**, *116*, 10703.

(24) Orr, J.; Ward, J. F. *Mol. Phys.* **1971**, *20*, 513.

(25) Frisch, M. J.; Trucks, G. W.; Schlegel, H. B.; Scuseria, G. E.; Robb, M. A.; Cheeseman, J. R.; Montgomery, J. A., Jr.; Vreven, T.; Kudin, K. N.; Burant, J. C.; Millam, J. M.; Iyengar, S. S.; Tomasi, J.; Barone, V.; Mennucci, B.; Cossi, M.; Scalmani, G.; Rega, N.; Petersson, G. A.; Nakatsuji, H.; Hada, M.; Ehara, M.; Toyota, K.; Fukuda, R.; Hasegawa, J.; Ishida, M.; Nakajima, T.; Honda, Y.; Kitao, O.; Nakai, H.; Klene, M.; Li, X.; Knox, J. E.; Hratchian, H. P.; Cross, J. B.; Adamo, C.; Jaramillo, J.; Gomperts, R.; Stratmann, R. E.; Yazyev, O.; Austin, A. J.; Cammi, R.; Pomelli, C.; Ochterski, W.; Ayala, P. Y.; Morokuma, K.; Voth, G. A.; Salvador, P.; Dannenberg, J. J.; Zakrzewski, V. G.; Dapprich, S.; Daniels, A. D.; Strain, M. C.; Farkas, O.; Malick, D. K.; Rabuck, A. D.; Raghavachari, K.; Foresman, J. B.; Ortiz, J. V.; Cui, Q.; Baboul, A. G.; Clifford, S.; Cioslowski, J.; Stefanov, B. B.; Liu, G.; Liashenko, A.; Piskorz, P.; Komaromi, I.; Martin, R. L.; Fox, D. J.; Keith, T.; Al-Laham, M. A.; Peng, C. Y.; Nanayakkara, A.; Challacombe, M.; Gill, P. M. W.; Johnson, B.; Chen, W.; Wong, M. W.; Gonzalez, C.; Pople, J. A. *Gaussian 03*, revision C.02 ed.; Gaussian, Inc.: Wallingford, CT, 2004.

(26) Becke, A. D. *J. Chem. Phys.* **1993**, *98*, 1372.

(27) Feller, D.; Davidson, E. R. Basis Sets for Ab Initio Molecular Orbital Calculations and Intermolecular Interactions. In *Reviews in Computational Chemistry*; Lipkowitz, K. B., Boyd, D. B., Eds.; VCH Publishers, Inc.: New York, 1990; Vol. 1, pp 1.

(28) van Gisbergen, S. J. A.; Schipper, P. R. T.; Gritsenko, O. V.; Baerends, E. J.; Snijders, J. G.; Champagne, B.; Kirtman, B. *Phys. Rev. Lett.* **1999**, *83*, 694.

(29) Jacquemin, D.; Perpete, E. A.; Andre, J.-M. *Int. J. Quant. Chem.* **2005**, *105*, 553.

(30) Liao, Y.; Eichinger, B. E.; Firestone, K. A.; Haller, M.; Luo, J.; Kaminsky, W.; Benedict, J. B.; Reid, P. J.; Jen, A. K. Y.; Dalton, L. R.; Robinson, B. H. *J. Am. Chem. Soc.* **2005**, *127*, 2758.

(31) Rehr, J. J. Personal communication.

(32) Gonze, X.; Ghosez, P.; Godby, R. W. *Phys. Rev. Lett.* **1995**, *74*, 4035.

(33) Bulat, F. A.; Toro-Labbe, A.; Champagne, B.; Kirtman, B.; Yang, W. *J. Chem. Phys.* **2005**, *123*, 014319.